

How does geometry affect quantum gases?

A. A. Araújo Filho^{1,*} and J. A. A. S. Reis^{2,3,†}

¹*Universidade Federal do Ceará (UFC), Departamento de Física,
Campus do Pici, Fortaleza – CE, C.P. 6030, 60455-760 - Brazil.*

²*Universidade Federal do Maranhão (UFMA), Departamento de Física,
Campus Universitário do Bacanga, São Luís – MA, 65080-805, Brazil*

³*Universidade Estadual do Maranhão (UEMA), Departamento de Física,
Cidade Universitária Paulo VI, São Luís – MA, 65055-310, Brazil*

(Dated: April 20, 2022)

Abstract

In this work, we study the thermodynamic functions of quantum gases confined to spaces of various shapes, namely, a sphere, a cylinder, and an ellipsoid. We start with the simplest situation, namely, a spinless gas treated within the canonical ensemble framework. As a next step, we consider *noninteracting* gases (fermions and bosons) with the usage of the grand canonical ensemble description. For this case, the calculations are performed numerically. We also observe that our results may possibly be applied to *Bose-Einstein condensate* and to *helium dimer*. Moreover, the bosonic sector, independently of the geometry, acquires entropy and internal energy greater than for the fermionic case. Finally, we also devise a model allowing us to perform analytically the calculations in the case of *interacting* quantum gases, and, afterwards, we apply it to a cubical box.

*Electronic address: dilto@fisica.ufc.br

†Electronic address: joao.andrade@discente.ufma.br

I. INTRODUCTION

The investigation of thermal aspects of materials has gained considerable attention in recent years especially in the context of condensed-matter physics and the development of new materials [1–4]. Given the existence of some well-known approximations, the electrons of a metal can be assumed to be a gas, as they are effectively free particles [5–10]. Such electron systems are worth exploring due to their relevance in fundamental [11, 12] and applied [13, 14] physical contexts. In parallel, a longstanding issue in quantum mesoscopic systems is how to perform an exact sum over the states of either *interacting* or *noninteracting* particles. Depending on the situation, the boundary effects cannot be neglected; instead, they should be taken into account in order to acquire a better agreement with the experimental results. Moreover, the properties of some systems are assumed to be shape dependent [15–17] and sensitive to their topology [18–22].

From a theoretical viewpoint, a related problem of statistical mechanics is to perform the sum over all accessible quantum states to obtain the physical quantities [23, 24]. Normally, the spectrum of particle states, which are confined in a volume, will be elucidated by the study of boundary effects. Nevertheless, if the particle wavelength is too short in comparison to the characteristic scale of the system under consideration, boundary effects can be overlooked. In previous years, such an assumption was supported by Rayleigh and Jeans in their radiation theory of electromagnetism [25]. Furthermore, such an involvement also emerged in a purely mathematical context and was rigorously solved afterwards by Weyl [26].

In this work, we study how the thermodynamic functions of quantum gases behave within different shapes, i.e., spherical, cylindrical, and ellipsoidal ones. Additionally, with possible experimental applications in mind, the thermodynamic functions are calculated for both *noninteracting* and *interacting* particles. Therefore, our results may help in the identification and in further studies involving geometry dependent phenomena within condensed-matter physics and statistical mechanics.

This paper is organized as follows. Initially, in Section II, we present a discussion involving the spectral energy for different geometries. Afterwards, in Section III, we focus on spinless particles using a setting of the canonical ensemble. Next, in Section IV, we focus on *noninteracting* gases (fermions and bosons) within the same geometries, using the grand

canonical ensemble instead. Moreover, in Section V, we propose two possible applications of our results, namely, the *Bose-Einstein condensate* and the *helium dimer*. Next, in Section VI, we devise a model to perform the calculation of *interacting* quantum gases which is applied to a cubical box. In contrast to the previous sections, the results are derived analytically. Finally, in Section VII, we conclude and discuss future perspectives.

II. SPECTRAL ENERGY FOR DIFFERENT GEOMETRIES

Initially, we study the thermodynamic properties of confined gases consisting of spinless particles. Moreover, fermions and bosons with a nonzero spin are also taken into account in our investigation. To do so, we must solve the Schrödinger equation for particular symmetries with appropriate boundary conditions. With this, the spectral energy can be derived after some algebraic manipulations. In particular, we choose three different geometries, namely, spherical, cylindrical, and ellipsoidal ones. The potentials for each configuration are given below:

$$\mathcal{V}_{\text{Sphere}}(r) = \begin{cases} 0, & \text{if } r < a \\ \infty, & \text{if } r > a \end{cases}, \quad (1a)$$

$$\mathcal{V}_{\text{Cylinder}}(\rho, z) = \begin{cases} 0, & \text{if } \rho < b \text{ and } 0 < z < 2c \\ \infty, & \text{otherwise} \end{cases}, \quad (1b)$$

$$\mathcal{V}_{\text{Ellipsoid}}(x, y, z) = \begin{cases} 0, & \text{if } x, y, z \text{ satisfy } \frac{x^2+y^2}{b^2} + \frac{z^2}{c^2} < 1 \\ \infty, & \text{if } x, y, z \text{ satisfy } \frac{x^2+y^2}{b^2} + \frac{z^2}{c^2} \geq 1 \end{cases}, \quad (1c)$$

where a , b and c are geometric parameters defining the size of the potential. In order to make a comparison between our thermodynamic results in the next sections, we must choose the parameters a , b , and c such that all configurations provide the same volume. Since we have already set up our potentials, we can solve the time-independent Schrödinger equation

$$-\frac{\hbar^2}{2M}\nabla^2\psi + V(r)\psi = E\psi, \quad (2)$$

for each geometry whose solutions can be obtained using the well-known method of separation of variables [25, 27–29]. Particularly, the wavefunction for the spherical case can be written as

$$\psi_{l,n,m}(r, \theta, \phi) = \begin{cases} A_{l,n} j_l(k_{l,n}r) Y_l^m(\theta, \phi), & \text{if } r \leq a \\ 0, & \text{if } r \geq a \end{cases}, \quad (3)$$

where $j_l(k_{l,n}r)$ is a spherical Bessel function, $Y_l^m(\theta, \phi)$ is a spherical harmonic and $A_{l,n}$ is a normalization factor; thereby, the Fourier transform of $\psi_{l,n,m}(r, \theta, \phi)$ is

$$\tilde{\psi}_{l,n,m}(k) = \frac{1}{\sqrt{(2\pi\hbar)^3}} A_{l,n} \int e^{i\mathbf{k}\cdot\mathbf{r}} j_l(k_{l,n}r) Y_l^m(\theta, \phi) r^2 dr d\Omega \quad (4)$$

and using the orthogonality properties of the Bessel functions [30–32], we can infer the momentum distribution $\tilde{n}(k)$

$$\tilde{n}(k) = s \sum_{l,n} |\tilde{\psi}_{l,n,m}(k)|^2 = \frac{3sV}{4\pi^2(\pi\hbar)^3} \sum_{l,n} (2l+1) j_l^2(ka) \frac{(k_{l,n}a/\pi)^2}{[(k_{l,n}a/\pi)^2 - (ka/\pi)^2]^2}, \quad (5)$$

where s is the spin degeneracy, $k_{l,n}a$ is the n -th root of $j_l(ka) = 0$, V is the volume, and k the momentum – it is considered to be continuous in the infinite volume limit. In Ref. [33], some approximations in order to perform analytical and numerical analyses of *noninteracting* particles at zero temperature were made. The shape dependence was investigated as well to see how such geometries would influence the momentum distribution $\tilde{n}(k)$. Our approach, on the other hand, intends to examine the impact of all mentioned shapes on the thermodynamic properties in comparison to the literature [16, 17]. To perform the following calculations, we consider spherical, cylindrical, and ellipsoidal configurations. Solving the Schrödinger equation for the spherical potential [27], we have

$$E_{n,l}^{\text{Sphere}} = (2l+1) \frac{\hbar^2}{2Ma^2} j_{nl}^2 \quad (6a)$$

where j_{nl} is the n -th zero of the l -th spherical Bessel function. Clearly, each level has a $(2l+1)$ -fold degeneracy. For ellipsoidal [28], cylindrical [27] shapes, we obtain

$$E_{m,n,l}^{\text{Ellipsoid}} = \frac{\hbar^2}{2M} \left[\frac{J_{n,l}^2}{b^2} + \frac{2J_{n,l}}{bc} \left(m + \frac{1}{2} \right) \right], \quad (6b)$$

$$E_{m,n,l}^{\text{Cylinder}} = \frac{\hbar^2}{2M} \left[\frac{J_{n,l}^2}{b^2} + \left(\frac{\pi m}{2c} \right)^2 \right]. \quad (6c)$$

where $J_{n,l}$ is the n -th root of the l -th Bessel function, and $n, m = 0, 1, \dots$. Using these spectral energies, an analysis of the thermal properties can properly be carried out in the next sections.

III. NONINTERACTING GASES: SPINLESS PARTICLES

In this section, we present the thermodynamic approach based on the canonical ensemble.

A. Thermodynamic approach

Whenever we are dealing with a spinless gas, the theory of the canonical ensemble is sufficient for a full thermodynamical description. Thereby, the partition function is given by

$$\mathcal{Z} = \sum_{\{\Omega\}} \exp(-\beta E_{\Omega}), \quad (7)$$

where Ω is related to accessible quantum states. Since we are dealing with *noninteracting* particles, the partition function (7) can be factorized which gives rise to the result below

$$\mathcal{Z} = \mathcal{Z}_1^N = \left\{ \sum_{\{\Omega\}} \exp(-\beta E_{\Omega}) \right\}^N, \quad (8)$$

where we have defined the single partition function as

$$\mathcal{Z}_1 = \sum_{\Omega} \exp(-\beta E_{\Omega}). \quad (9)$$

It is known that the thermodynamical description of the system can also be done via Helmholtz free energy

$$f = -\frac{1}{\beta} \lim_{N \rightarrow \infty} \frac{1}{N} \ln \mathcal{Z}, \quad (10)$$

where rather for convenience we write the Helmholtz free energy per particle. With this, we can derive the following thermodynamic state functions¹, i.e., entropy, heat capacity, and mean energy

$$s = -\frac{\partial f}{\partial T}, \quad (11a)$$

$$c = T \frac{\partial s}{\partial T}, \quad (11b)$$

and

$$u = -\frac{\partial}{\partial \beta} \ln \mathcal{Z}. \quad (11c)$$

The sum in Eq. (9) cannot be expressed in a closed form. This does not allow us to proceed analytically. To overcome this issue, we perform a numerical analysis plotting the respective functions in terms of the temperature in order to understand their behaviors. Our main interest lies in the study of the low-temperature regime.

¹ All of them are written in a “per particle form” for convenience.

| | | a | b | c |
|-----------|-----------|-----|------|------|
| Config. 1 | Sphere | 1.0 | - | - |
| | Cylinder | - | 1.0 | 0.66 |
| | Ellipsoid | - | 1.22 | 0.66 |
| Config. 2 | Sphere | 1.5 | - | - |
| | Cylinder | - | 1.22 | 1.5 |
| | Ellipsoid | - | 1.67 | 1.2 |

Table I: The parameters a , b and c for two distinct configurations.

B. Numerical analysis

To provide the numerical results below, we sum over fifty thousand terms in Eq. (9). With this, we can guarantee the accuracy of such procedure keeping the maximum of details. For the plots below, the values for the parameters a , b and c^2 , that control the size of the potential, are displayed in Tab. I. For now on, we will refer to the first set of parameters as configuration 1 (thick lines in the plots) and to the second set as configuration 2 (dashed lines in the plots). Note that configuration 2 has a larger volume than configuration 1. However, the parameters are chosen such that the wells considered (sphere, cylinder and ellipsoid) have the same volume in each configuration. We also need to mention that we are using the mass of the electron $M = 0.5$ MeV in order to provide the numerical results. The graphics for the configurations described here are displayed in Fig. 1

Let us start by analyzing the Helmholtz free energy. In Fig. 1, we see that configuration 1 provides larger values of the Helmholtz free energy than configuration 2. Besides, we also see that the values of the energy are larger for the sphere in comparison to the ellipsoid; and the latter one is larger in comparison to the cylinder for both configurations. In what follows, we will employ the short-hand notation $Sphere > Ellipsoid > Cylinder$. The behavior of the entropy, on the other hand, seems to be different. We notice that configuration 2 provides an entropy larger than configuration 1 and, when we look at the geometry itself, we observe

² The unit chosen for these parameters in the table is the nanometer. In units of the reduced Compton wavelength, we must remember the conversion factor $1 \text{ nm} = 2.58 \times 10^3 \lambda$. With this information, it is easy to perform the conversion between these units.

the pattern $Cylinder > Ellipsoid > Sphere$. In this comparison, the *Ellipsoidal* geometry always takes a position in the middle. This fact is expected since this geometry is actually a “transition” between a cylinder and a sphere.

Also in Fig. 1, we find the plots for the internal energy and for the heat capacity. Configuration 1 exhibits energies larger than those of configuration 2 and we see that the internal energy increases according to $Sphere > Ellipsoid > Cylinder$ for both configurations. The heat capacities for all configurations approach the value $3/2$ as the temperature increases. Configuration 2, that has a larger volume, reaches the asymptotic value faster than configuration 1.

Differently from what we saw for the other thermodynamic quantities, it is not possible to establish a common behavior among *Ellipsoid*, *Cylinder* and *Sphere* geometries because of different temperature ranges and well sizes the heat capacity varies drastically. For instance, in the second row of Fig. 1, configuration 2 in the range $0 < T < 5$ K, we see that the heat capacity follows the rule $Ellipsoid > Cylinder > Sphere$. However, in the same range of temperature, configuration 1 displays two different behaviors, i.e., for $0 < T < 2.5$ K, we have $Cylinder > Ellipsoid > Sphere$ and for $2.5 \text{ K} < T < 5 \text{ K}$, we have $Ellipsoid > Cylinder > Sphere$. For a fixed value of the volume, there exists a temperature where the heat capacity will follow the rule $Sphere > Ellipsoid > Cylinder$ until it reaches the value $3/2$. This temperature increases as the volume decreases. For configuration 1, the temperature where we have this behavior is around 29 K and, for configuration 2, it happens at 9 K.

It is interesting to see that for the cylindrical geometry a mound appears around 0.5 K and tends to disappear when the volume of the cylinder increases. This effect is clearly caused by the finite size of the geometry since the expected behavior would be to go to zero almost linearly. However, both the sphere and the ellipsoid do not exhibit such an effect. We could conclude about the absence of such effect that the surfaces of the former cases that accentuate those geometries are smooth and the cylinder, on the other hand, is smooth just by parts. As we will see in Sec. VI and in Ref. [17], it is possible to identify the contribution that comes from the geometry itself by considering an analytical model.

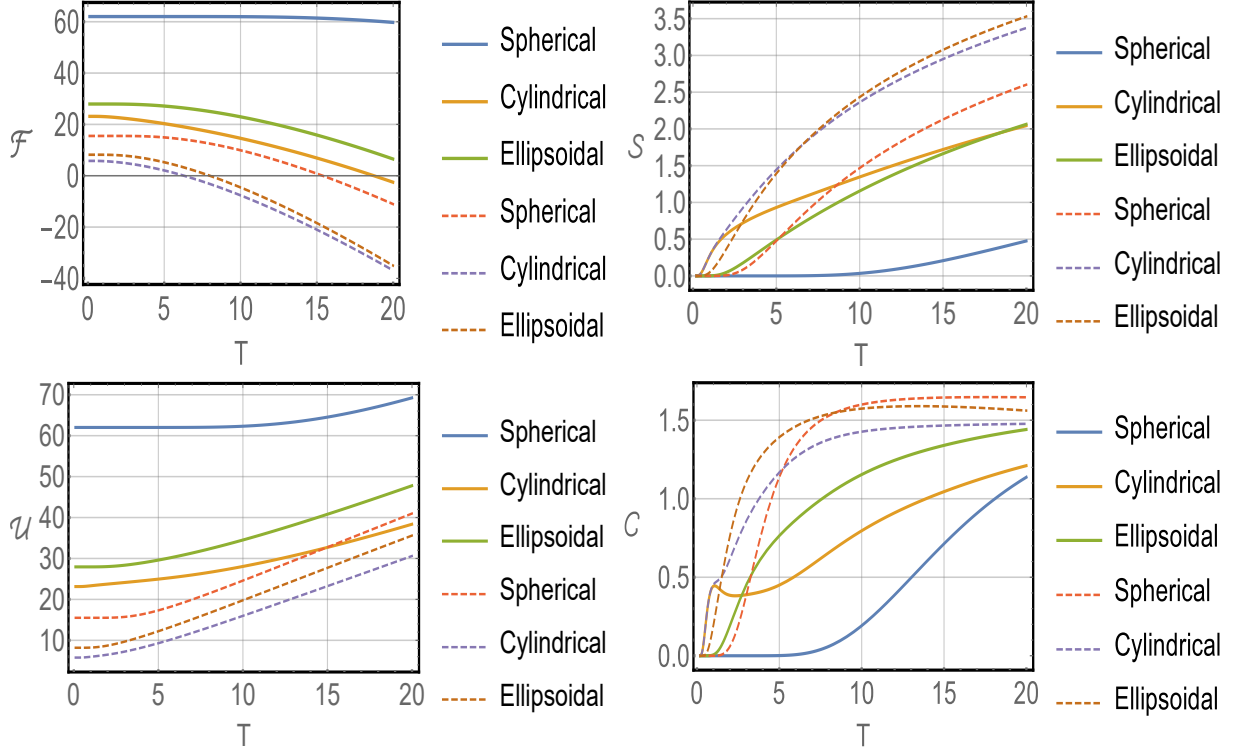


Figure 1: The Helmholtz free energy, entropy per particle, the internal energy and heat capacity per particle, respectively

IV. NONINTERACTING GASES: BOSONS AND FERMIONS

Although interactions of atoms and molecules are treated in many experimental approaches, and several features may only be recognized and understood by taking the interactions into account [34–37], some fascinating characteristics are well described by assuming *noninteracting* systems [38–50].

Studies of *noninteracting* particles (bosons and fermions) have many applications, especially in chemistry [48, 49] and condensed-matter physics [38–47, 50, 51]; for instance, in the case of *bulk*, which is usually assumed to calculate the energy spectrum and use the *Fermi-Dirac* distribution to examine how its statistics behaves, it is sufficient to describe the system of a *noninteracting* electron gas. Such an assumption is totally reasonable since if the *Fermi energy* is large enough, the kinetic energy of electrons, close to the Fermi level, will be much greater than the potential energy of the *electron-electron* interaction.

On the other hand, one of the pioneer studies which addressed the analysis of the *Bose-Einstein condensate* in a theoretical viewpoint was presented in [52]. The authors utilize a

gas of *noninteracting* bosons to perform their calculations. As we shall see, we proceed in a similar way taking into account different geometries. Furthermore, we discuss applying them in different scenarios in condensed-matter physics.

A. Thermodynamic approach

We apply the grand canonical ensemble theory to *noninteracting* particles with different spins (fermions and bosons); we will treat both cases separately. The grand canonical partition function for the present problem reads

$$\Xi = \sum_{N=0}^{\infty} \exp(\beta\mu N) \mathcal{Z}[N_{\Omega}], \quad (12)$$

where $\mathcal{Z}[N_{\Omega}]$ is the usual canonical partition function which now depends on the occupation number N_{Ω} , and on μ , which is the chemical potential. Since we are dealing with fermions and bosons, it is well-known that the occupation number must be restricted in the following manner: $N_{\Omega} = \{0, 1\}$ for fermions and $N_{\Omega} = \{0, \dots, \infty\}$ for bosons. Also, for an arbitrary quantum state, the energy depends on the occupation number as

$$E\{N_{\Omega}\} = \sum_{\{\Omega\}} N_{\Omega} E_{\Omega}$$

where we have

$$\sum_{\{\Omega\}} N_{\Omega} = N.$$

In this way, the partition function becomes

$$\mathcal{Z}[N_{\Omega}] = \sum_{\{N_{\Omega}\}} \exp\left[-\beta \sum_{\{\Omega\}} N_{\Omega} E_{\Omega}\right], \quad (13)$$

which leads to

$$\Xi = \sum_{N=0}^{\infty} \exp(\beta\mu N) \sum_{\{N_{\Omega}\}} \exp\left[-\beta \sum_{\{\Omega\}} N_{\Omega} E_{\Omega}\right], \quad (14)$$

or can be rewritten as

$$\Xi = \prod_{\{\Omega\}} \left\{ \sum_{\{N_{\Omega}\}} \exp[-\beta N_{\Omega} (E_{\Omega} - \mu)] \right\}. \quad (15)$$

After performing the sum over the possible occupation numbers, we get

$$\Xi = \prod_{\{\Omega\}} \{1 + \chi \exp[-\beta(E_\Omega - \mu)]\}^\chi, \quad (16)$$

where we have now introduced the convenient notation $\chi = +1$ for fermions and $\chi = -1$ for bosons. The connection with thermodynamics is made by using the grand thermodynamical potential given by

$$\Phi = -\frac{1}{\beta} \ln \Xi. \quad (17)$$

Replacing Ξ in the above equation, we get

$$\Phi = -\frac{\chi}{\beta} \sum_{\{\Omega\}} \ln \{1 + \chi \exp[-\beta(E_\Omega - \mu)]\}. \quad (18)$$

The entropy of the system can be cast into the following compact form, namely

$$S = -\frac{\partial \Phi}{\partial T} = -k_B \sum_{\{\Omega\}} \mathcal{N}_\Omega \ln \mathcal{N}_\Omega + \chi (1 - \chi \mathcal{N}_\Omega) \ln (1 - \chi \mathcal{N}_\Omega)$$

where

$$\mathcal{N}_\Omega = \frac{1}{\exp[\beta(E_\Omega - \mu)] + \chi}.$$

Moreover, we can also use the grand potential to calculate other thermodynamic properties, such as, the mean particle number, energy, heat capacity, and pressure using the following expressions:

$$\mathcal{N} = -\frac{\partial \Phi}{\partial \mu}, \quad (19a)$$

$$\mathcal{U} = -T^2 \frac{\partial}{\partial T} \left(\frac{\Phi}{T} \right), \quad (19b)$$

$$C = T \frac{\partial S}{\partial T}, \quad (19c)$$

$$\mathcal{P} = -\frac{\partial \Phi}{\partial V} = -\frac{\Phi}{V}. \quad (19d)$$

In possession of these terms, calculating the thermodynamic quantities should be a straightforward task, since we would only need to perform the sum presented in Eq. (18). Unfortunately, this sum cannot be obtained in a closed form for the spectral energy that we chose. Instead of this, a numerical analysis, similar to that shown in Sec. III B, can be performed to overcome this difficulty; thereby, we can obtain the behavior of all quantities considering mainly the low temperature regimes (keeping the volume constant). In what follows, we present the results of our numerical studies.

B. Numerical analysis

Here, as in Section III B, we consider two particular cases whose parameters are the same as those presented in Tab. I. For numerical purpose, we choose for the chemical potential the value $\mu = 0.5$ eV and, again, $M = 0.5$ MeV. Next, we also use thick and dashed lines to represent fermions and bosons in the plots presented in Fig. 2. In the first row of Fig. 2, we present the entropy for the two different cases. The first one, in Fig. 2a, represents configuration 1 and Fig. 2b configuration 2, where we compare fermions (thick lines) and bosons (dashed lines) for sphere, cylinder and ellipsoid geometries. We can see from the plots that bosons, independently of the previous set of geometry we chose, acquire an entropy larger than fermions. We can also realize that the pattern *Ellipsoid* > *Cylinder* > *Sphere* always occurs for fermions and bosons when we consider the entropy. In both cases, the pattern described above repeats and shows that the entropy is a monotonically increasing function for volume and temperature.

For the internal energy, displayed in the second row Fig. 2, we see the entire behavior being repeated, namely, the internal energy follows the rule *Ellipsoid* > *Cylinder* > *Sphere* and the energy for bosons are greater than for fermions when we compare their values for the same geometry. It is also important to notice that the internal energy is a monotonically increasing function for both volume and temperature.

Another important property analyzed here is the heat capacity showed in the third row of Fig. 2. We know from the literature [23, 24] that the heat capacity for an electron gas at low temperature ($T \ll T_{Fermi}$) is proportional to the temperature. On the other hand, for the boson gas, the heat capacity is proportional to $T^{3/2}$ (both behaviors are obtained in the classical limit). However, as we can deduce from the graphics, in both cases presented in Fig. 2, fermions do not follow this rule. We see deviations from a straight line, where one can infer that this effect is caused by the finite volume. We must remember that our systems are under confinement in very small containers³ and, in addition, a large number of energy levels were considered in the numerical analysis. As a direct consequence, the entire behavior at low temperature, when compared to the usual electron gas, will be drastically different. On

³ The linear dimension of the containers considered is comparable with the thermal wavelength of the electron for low temperatures. This means that the electrons will feel the finiteness of the well and, therefore, the thermodynamic properties will change.

the other hand, bosons behave exactly like a function proportional to $T^{3/2}$. It suggests that fermions are more sensitive to the geometry and size of the system than bosons. Besides the discussion above, we can also see that in general the heat capacity follows the pattern *Ellipsoid* > *Cylinder* > *Sphere* and its value increases when both temperature and volume increase.

V. FURTHER APPLICATIONS: NONINTERACTING GASES

In this section, we address qualitatively some possible future applications of our *non-interacting* model for quantum gases developed so far. In particular, we look toward the *Bose-Einstein condensate* and the *helium dimer*.

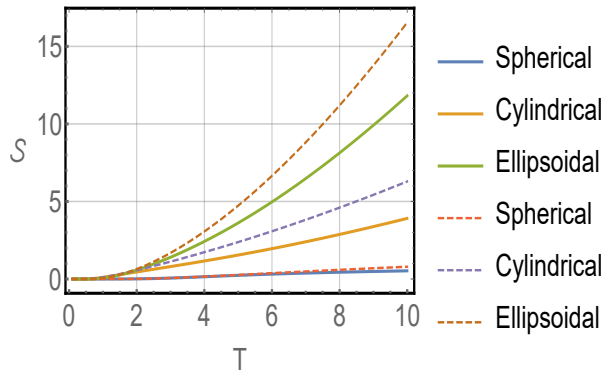
A. Bose-Einstein condensate

In Ref. [52], the grand canonical ensemble is also used to perform the calculations; the authors studied the asymptotic behavior of various thermodynamic and statistical quantities related to a confined ideal *Bose-Einstein* gas. In this case, the considered object is an arbitrary, finite, cubical enclosure subjected to periodic boundary conditions, i.e., thin-film, square-channel and cubic geometries.

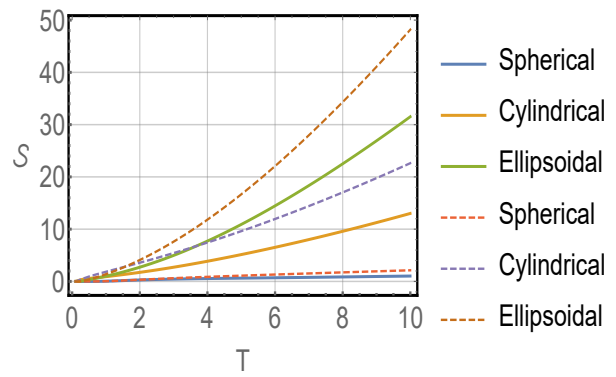
Following the approach of Ref. [52], our proposition is to probe how the thermal quantities are affected by spherical, cylindrical, and ellipsoidal geometries. This study can be useful within a possible future experimental scenario to be studied in material science.

B. Helium atoms - ^3He and ^4He

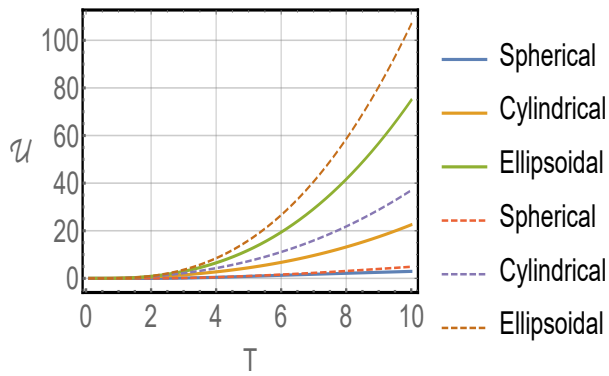
Taking the advantage of solving the Schrödinger equation numerically as well as the construction of suitable wavefunctions, in Refs. [53, 54], the binding of two helium atoms involving restricted and unrestricted geometries was studied in two and three dimensions. Such a model describes two atoms placed in a spherical potential (1a) with hard walls. As argued, one could insert a nontrivial interaction of the helium atoms with the walls [55–58] and also some coupling between them, as presented in Sec. VI. Nevertheless, the interaction of the particles with the wall depends on the material of the cavity. Thereby, it is feasible to



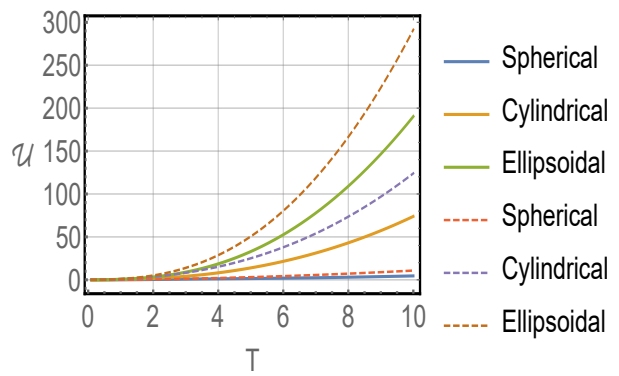
(a) Entropy case 1



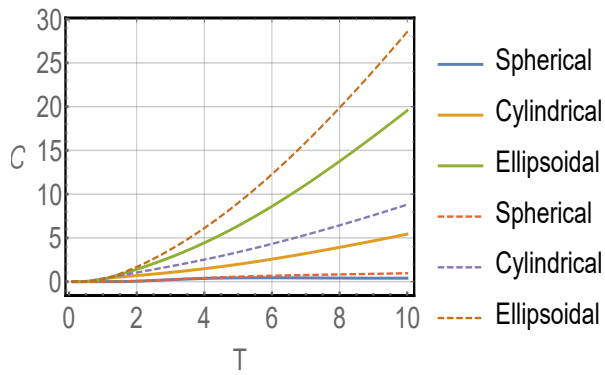
(b) Entropy case 2



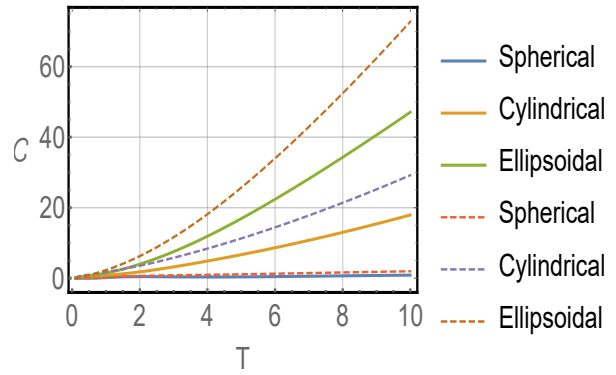
(c) Energy case 1



(d) Energy case 2



(e) Heat capacity case 1



(f) Heat capacity case 2

Figure 2: The different behaviors for the entropy, mean energy and heat capacity, respectively

propose a general investigation of these phenomena rather than being limited to individual cases.

In this sense, our proposal is as follows: based on the relevance of studying either helium liquids or helium dimer in solid matrices, a study of how geometry influences the thermodynamic properties of such constrained systems might be relevant for future applications in condensed matter physics. Likewise, for the cylindrical shape (1b), it is notable to aim at investigating the thermal properties of shapes similar to that of carbon nanotubes [59, 60]. Also, using some approximations, vortex-like shapes [61, 62] could reasonably be examined as well.

VI. INTERACTING GASES: AN ANALYTICAL APPROACH

A. The model

We intend now to take into account interactions between particles. To do so, we modify slightly the approach developed in Sec. IV by introducing an interaction term $U(V, n)$. Here, we assume that the interaction energy depends only on the particle density n and the volume V . As demonstrated below, such a type of interaction appears in the mean field approximation, and enables us to derive analytical results. Furthermore, as we shall verify, these solutions will allow us to recognize how the interactions can modify the thermal quantities of our system. It is important to highlight that the interaction term is a monotonically increasing function of the particle density. Thereby, if the density n is increased, the particles will come closer to each other and the respective interactions between them are supposed to increase. Analogously, the opposite behavior happens otherwise: if n decreases, $U(V, n)$ will have to decrease. Throughout this section, we adopt natural units where $k_B = 1$. Doing that, we get the following grand canonical partition function

$$\mathcal{Z}(T, V, \mu) = \sum_{\{N_\Omega\}=0}^{\{\infty/1\}} z^N \exp \left\{ -\beta \left[\sum_{\{\Omega\}} N_\Omega (E_\Omega) + U(V, n) \right] \right\}, \quad (20a)$$

where

$$z^N = \exp \{N\beta\mu\} = \exp \left\{ \beta \sum_{\{\Omega\}} N_\Omega \mu \right\}. \quad (20b)$$

The sum index which appears in Eq. (20a), namely $\{\infty/1\}$, shows that infinitely many bosons may occupy the same quantum state Ω . On the other hand, if one considers instead of this, spin-half particles, only one fermion will be allowed due to the Pauli exclusion principle. In a compact notation, we take the upper index ∞ for bosons and 1 for fermions. Let us now suppose that the interaction term has the form $U(V, n) = Vu(n)$. With this, we have

$$\mathcal{Z}(T, V, \mu) = \sum_{\{N_\Omega\}=0}^{\{\infty/1\}} \exp \left\{ -\beta \left[\sum_{\{\Omega\}} N_\Omega (E_\Omega - \mu) + Vu(n) \right] \right\}. \quad (21)$$

For the sake of simplicity, in Eq. (21), we assume that $Vu(n)$ is linear in $\sum_\Omega N_\Omega = N$. Furthermore, the only appropriate manner to do so is to linearize $Vu(n)$. To do that, we use the Taylor series expansion of $u(n)$ around the mean value \bar{n} :

$$u(n) = u(\bar{n}) + u'(\bar{n})(n - \bar{n}) + \dots \quad (22)$$

More so, if one regards that the potential energy is dependent on the position that the particles occupy, Eq. (22) will account for the *molecular field approximation*. Such assumption is vastly employed in the literature concerning for instance condensed matter physics [63–68]. Thereby, we can derive the energy of the quantum state Ω as being

$$E = \sum_{\{\Omega\}} N_\Omega [E_\Omega + u'(\bar{n})] + U(V, \bar{n}) - u'(\bar{n})\bar{N}, \quad (23)$$

and the summation of Eq. (21) can be evaluated

$$\begin{aligned} \mathcal{Z}(T, V, \mu) &= \exp \left\{ -\beta [U(V, \bar{n}) - u'(\bar{n})\bar{N}] \right\} \\ &\times \prod_{\Omega=1}^{\infty} \left(\sum_{N_\Omega=0}^{\{\infty/1\}} \exp \left\{ -\beta [E_\Omega + u'(\bar{n}) - \mu] N_\Omega \right\} \right). \end{aligned} \quad (24)$$

After some algebraic manipulations, we can present the above expression as

$$\begin{aligned} \mathcal{Z}(T, V, \mu) &= \exp \left\{ -\beta [U(V, \bar{n}) - u'(\bar{n})\bar{N}] \right\} \\ &\times \prod_{\Omega=1}^{\infty} \begin{cases} 1 + \exp[-\beta(E_\Omega + u'(\bar{n}) - \mu)], \text{ fermions} \\ (1 - \exp[-\beta(E_\Omega + u'(\bar{n}) - \mu)])^{-1}, \text{ bosons} \end{cases}, \end{aligned} \quad (25)$$

or in a more compact form

$$\begin{aligned} \mathcal{Z}(T, V, \mu) &= \exp \left\{ -\beta [U(V, \bar{n}) - u'(\bar{n})\bar{N}] \right\} \\ &\times \prod_{\Omega=1}^{\infty} (1 + \chi \exp[-\beta(E_\Omega + u'(\bar{n}) - \mu)])^\chi, \end{aligned} \quad (26)$$

where $\chi = 1$ for fermions, and $\chi = -1$ for bosons.

B. Thermodynamic state quantities

Next, the derivation of the grand canonical potential is straightforward as follows

$$\begin{aligned}\Phi &= -T \ln \mathcal{Z} \\ &= -T\chi \sum_{\Omega} \ln (1 + \chi \exp [-\beta (E_{\Omega} + u'(\bar{n}) - \mu)]) + U(V, \bar{n}) - u'(\bar{n}) \bar{N}.\end{aligned}\quad (27)$$

Based on this equation, the other thermodynamic functions can be calculated as well. In this sense, the mean particle number reads

$$\begin{aligned}\bar{N} &= - \left. \frac{\partial \Phi}{\partial \mu} \right|_{T,V}, \\ &= -V \left. \frac{\partial u(\bar{n})}{\partial \mu} \right|_{T,V} + \bar{N} \left. \frac{\partial u'(\bar{n})}{\partial \mu} \right|_{T,V} + u'(\bar{n}) \left. \frac{\partial \bar{N}}{\partial \mu} \right|_{T,V} + \\ &\quad + T\chi \sum_{\Omega} \frac{\chi \exp [-\beta (E_{\Omega} + u'(\bar{n}) - \mu)]}{1 + \chi \exp [-\beta (E_{\Omega} + u'(\bar{n}) - \mu)]} \beta \left(1 - \left. \frac{\partial u'(\bar{n})}{\partial \mu} \right|_{T,V} \right),\end{aligned}\quad (28)$$

and from this,

$$\begin{aligned}\bar{N} \left(1 - \left. \frac{\partial u(\bar{n})}{\partial \mu} \right|_{T,V} \right) &= -V \left. \frac{\partial u(\bar{n})}{\partial \mu} \right|_{T,V} + u'(\bar{n}) \left. \frac{\partial \bar{N}}{\partial \mu} \right|_{T,V} \\ &\quad + \chi^2 \beta T \left(1 - \left. \frac{\partial u'(\bar{n})}{\partial \mu} \right|_{T,V} \right) \sum_{\Omega} \frac{1}{\exp [\beta (E_{\Omega} + u'(\bar{n}) - \mu)] + \chi}.\end{aligned}\quad (29)$$

Since

$$\left. \frac{\partial u(\bar{n})}{\partial \mu} \right|_{T,V} = u'(\bar{n}) \left. \frac{\partial \bar{n}}{\partial \mu} \right|_{T,V} = \frac{u'(\bar{n})}{V} \left. \frac{\partial \bar{N}}{\partial \mu} \right|_{T,V},\quad (30)$$

we get

$$\bar{N} = \sum_{\Omega} \frac{1}{\exp [\beta (E_{\Omega} + u'(\bar{n}) - \mu)] + \chi}.\quad (31)$$

The mean occupation number must be $\bar{N} = \sum_{\Omega} \bar{n}_{\Omega}$, where

$$\bar{n}_{\Omega} = \frac{1}{\exp [\beta (E_{\Omega} + u'(\bar{n}) - \mu)] + \chi}.\quad (32)$$

As we can also notice that the interaction modifies the mean particle number since the term $u'(\bar{n})$ is present in Eq. (32). This modification is directly related to the fact that we chose the interaction energy to be a function of the particle density.

Next, the entropy is given by

$$S = - \left. \frac{\partial \Phi}{\partial T} \right|_{\mu,V},$$

$$\begin{aligned}
&= -V \left. \frac{\partial u(\bar{n})}{\partial T} \right|_{\mu, V} + \bar{N} \left. \frac{\partial u'(\bar{n})}{\partial T} \right|_{\mu, V} + u'(\bar{n}) \left. \frac{\partial \bar{N}}{\partial T} \right|_{\mu, V} \\
&+ \chi \sum_{\Omega} \ln(1 + \chi \exp[-\beta(E_{\Omega} + u'(\bar{n}) - \mu)]) \\
&+ \chi^2 T \sum_{\Omega} \frac{(E_{\Omega} + u'(\bar{n}) - \mu) \left(-\frac{d\beta}{dT}\right) - \beta \left. \frac{\partial u'(\bar{n})}{\partial T} \right|_{\mu, V}}{\exp[\beta(E_{\Omega} + u'(\bar{n}) - \mu)] + \chi}, \tag{33}
\end{aligned}$$

or in a more compact form,

$$\begin{aligned}
S &= \chi \sum_{\Omega} \ln(1 + \chi \exp[-\beta(E_{\Omega} + u'(\bar{n}) - \mu)]) \\
&+ \frac{1}{T} \sum_{\Omega} \bar{n}_{\Omega} (E_{\Omega} + u'(\bar{n}) - \mu). \tag{34}
\end{aligned}$$

Moreover, the mean energy reads

$$\begin{aligned}
\bar{E} &= \left. \frac{\partial(\beta\Phi)}{\partial\beta} \right|_{z, V}, \\
&= \left. \frac{\partial}{\partial\beta} [\beta V u(\bar{n}) - \beta \bar{N} u'(\bar{n})] \right|_{z, V} \\
&- \chi \sum_{\Omega} \frac{\chi z \exp[-\beta(E_{\Omega} + u'(\bar{n}))]}{1 + \chi z \exp[-\beta(E_{\Omega} + u'(\bar{n}))]} \left(-E_{\Omega} - \left. \frac{\partial}{\partial\beta} [\beta u'(\bar{n})] \right|_{z, V} \right), \\
&= U(V, \bar{n}) + \beta V \left. \frac{\partial u(\bar{n})}{\partial\beta} \right|_{z, V} - \bar{N} \left. \frac{\partial [\beta u'(\bar{n})]}{\partial\beta} \right|_{z, V} - \beta u'(\bar{n}) \left. \frac{\partial \bar{N}}{\partial\beta} \right|_{z, V} \\
&+ \sum_{\Omega} \frac{E_{\Omega}}{z^{-1} \exp[\beta(E_{\Omega} + u'(\bar{n}))] + \chi} + \bar{N} \left. \frac{\partial [\beta u'(\bar{n})]}{\partial\beta} \right|_{z, V}. \tag{35}
\end{aligned}$$

After some algebraic manipulations, one can rewrite this expression as

$$\bar{E} = \sum_{\Omega} \bar{n}_{\Omega} E_{\Omega} + U(V, \bar{n}). \tag{36}$$

This is an expected result since the energy is the average of the kinetic term plus the interactions energy. Finally, we derive the pressure of the system

$$\begin{aligned}
p &= - \left. \frac{\partial\Phi}{\partial V} \right|_{\mu, T}, \\
&= -u(\bar{n}) + u'(\bar{n}) \left. \frac{\partial \bar{N}}{\partial V} \right|_{\mu, T} + \frac{\chi T}{V} \sum_{\Omega} \ln(1 + \chi \exp[-\beta(E_{\Omega} + u'(\bar{n}) - \mu)]), \tag{37}
\end{aligned}$$

$$= -\frac{\Phi}{V}, \tag{38}$$

where we have used Eq. (31) and the fact that the particle density does not depend on the volume. From Eq. (37), we can also realize how interaction plays an important role on the pressure. The first term in Eq. (37), $-u(\bar{n})$, for instance, is responsible to reduce the pressure of the system, while the second one, $u'(\bar{n})$, plays the role of increasing it instead. It is worth mentioning that such thermal functions were recently calculated in [69–75] for Lorentz-violating systems.

C. Analytical results for three-dimensional boxes

We exemplify our model constructed above for the three-dimensional box. The spectral energy is

$$E_{\eta_x, \eta_y, \eta_z}^{\text{Box}} = \frac{\pi^2 \hbar^2}{2M} \left(\frac{\eta_x^2}{L_x^2} + \frac{\eta_y^2}{L_y^2} + \frac{\eta_z^2}{L_z^2} \right). \quad (39)$$

Here, the grand canonical potential of an *interacting* gas is

$$\Phi = -k_B T \chi \sum_{\{\eta_x, \eta_y, \eta_z\}} \ln \left\{ 1 + \chi \exp \left[-\beta \left(E_{\eta_x, \eta_y, \eta_z}^{\text{Box}} + u'(\bar{n}) - \mu \right) \right] \right\} + U(V, \bar{n}) - u'(\bar{n}) \bar{N}. \quad (40)$$

To proceed further, the *Euler–MacLaurin formula* [21, 76, 77] must be utilized,

$$\begin{aligned} \sum_n F(n) &= \int_0^\infty F(n) dn + \frac{1}{2} F(0) \\ &\quad - \frac{1}{2!} B_2 F'(0) - \frac{1}{4!} B_4 F'''(0) + \dots, \end{aligned} \quad (41)$$

where B'_k s are the Bernoulli numbers. This allows us to approximate Φ , for low- T regime⁴, as:

$$\begin{aligned} \Phi &\approx -k_B T \chi \int_0^\infty \int_0^\infty \int_0^\infty d\eta_x d\eta_y d\eta_z \ln \left\{ 1 + \chi \mathfrak{z} \exp \left[-\beta E_{\eta_x, \eta_y, \eta_z}^{\text{Box}} \right] \right\} \\ &\quad + \frac{k_B T \chi}{2} \int_0^\infty \int_0^\infty d\eta_y d\eta_z \ln \left\{ 1 + \chi \mathfrak{z} \exp \left[-\beta E_{0, \eta_y, \eta_z}^{\text{Box}} \right] \right\} \\ &\quad + \frac{k_B T \chi}{2} \int_0^\infty \int_0^\infty d\eta_x d\eta_z \ln \left\{ 1 + \chi \mathfrak{z} \exp \left[-\beta E_{\eta_x, 0, \eta_z}^{\text{Box}} \right] \right\} \\ &\quad + \frac{k_B T \chi}{2} \int_0^\infty \int_0^\infty d\eta_x d\eta_y \ln \left\{ 1 + \chi \mathfrak{z} \exp \left[-\beta E_{\eta_x, \eta_y, 0}^{\text{Box}} \right] \right\} \end{aligned}$$

⁴ The higher order terms become negligible because the low temperature regime under consideration makes the exponential function very small in Eq. (40). The higher order corrections become relevant for high- T regime. On the other hand, for low- T regime, we can estimate $T < 100$ K.

$$\begin{aligned}
& + \frac{k_B T \chi}{4} \int_0^\infty d\eta_x \ln \left\{ 1 + \chi \mathfrak{z} \exp \left[-\beta E_{\eta_x, 0, 0}^{\text{Box}} \right] \right\} \\
& + \frac{k_B T \chi}{4} \int_0^\infty d\eta_y \ln \left\{ 1 + \chi \mathfrak{z} \exp \left[-\beta E_{0, \eta_y, 0}^{\text{Box}} \right] \right\} \\
& + \frac{k_B T \chi}{4} \int_0^\infty d\eta_z \ln \left\{ 1 + \chi \mathfrak{z} \exp \left[-\beta E_{0, 0, \eta_z}^{\text{Box}} \right] \right\} \\
& + \frac{k_B T \chi}{8} \ln(1 + \chi \mathfrak{z}) + U(V, \bar{n}) - u'(\bar{n}) \bar{N}, \tag{42}
\end{aligned}$$

where we have defined $\mathfrak{z} = z e^{-\beta u'(\bar{n})}$. After performing the integrals, we obtain

$$\Phi = \frac{\mathcal{V}}{\lambda^3} h_{\frac{5}{2}}(\mathfrak{z}) - \frac{1}{4} \frac{\mathcal{S}}{\lambda^2} h_2(\mathfrak{z}) + \frac{1}{16} \frac{\mathcal{L}}{\lambda} h_{\frac{3}{2}}(\mathfrak{z}) - \frac{1}{8} h_1(\mathfrak{z}) + U(V, \bar{n}) - u'(\bar{n}) \bar{N}, \tag{43}$$

where $\lambda = h/\sqrt{2\pi M k_B T}$ is the thermal wavelength, $\mathcal{V} = L_x L_y L_z$ is the volume, $\mathcal{S} = 2(L_x L_y + L_y L_z + L_z L_x)$ the area of the surface, $\mathcal{L} = 4(L_x + L_y + L_z)$ the total length of the edges of the box and

$$h_\sigma(\mathfrak{z}) = \frac{1}{\Gamma(\sigma)} \int_0^\infty \frac{t^{\sigma-1}}{\mathfrak{z}^{-1} e^t + \chi} dt = \begin{cases} f_\sigma(\mathfrak{z}), & \text{for fermions } (\chi = 1) \\ g_\sigma(\mathfrak{z}), & \text{for bosons } (\chi = -1) \end{cases}. \tag{44}$$

The boundary effects in Eq. (43) are represented by the second and third terms which are proportional to the perimeter \mathcal{L} and to the surface \mathcal{S} . We note that these terms are modified by the interaction term $u'(\bar{n})$. Also, we can carry out a similar calculation involving a two-dimensional box.

As an application, let us use the result obtained from Eq. (43) to probe how interaction affects the Fermi energy. From that, we get

$$N = g \left[\frac{V}{\lambda^3} f_{\frac{3}{2}}(\mathfrak{z}) - \frac{1}{4} \frac{\mathcal{S}}{\lambda^2} f_1(\mathfrak{z}) + \frac{L}{16\lambda} f_{\frac{1}{2}}(\mathfrak{z}) - \frac{1}{8} \frac{\mathfrak{z}}{\mathfrak{z} + 1} \right], \tag{45}$$

where g is a weight factor that arises from the internal structure of the particles. The Fermi energy μ_0 is the energy of the topmost filled level in the ground state of an electron system. In this way,

$$N = g \left[\frac{V}{6\pi^2} \left(\frac{2m\mathfrak{X}}{\hbar^2} \right)^{\frac{3}{2}} - \frac{1}{4} \frac{\mathcal{S}}{4\pi} \left(\frac{2m\mathfrak{X}}{\hbar^2} \right) + \frac{L}{16\pi} \left(\frac{2m\mathfrak{X}}{\hbar^2} \right)^{\frac{1}{2}} - \frac{1}{8} \right], \tag{46}$$

where $\mathfrak{X} = \mu_0 - u'(n)$. The Fermi energy cannot be calculated from this equation until we conveniently choose the interaction $u(n)$ term. However, we can at least see how the interaction modifies the structure of the equation which determines the Fermi energy μ_0 .

It is also possible to infer that the existence of an interaction enhances such energy level. Moreover, we realize that the interaction remarkably introduces a density-dependence on the Fermi energy. Unfortunately, even for a linear approximation, it is not possible to get an analytical result for μ_0 . On the other hand, Eq. (46) give us an idea of the challenge that we have to face in order to solve μ_0 numerically.

Finally, a straightforward question is worthy to be taken into account: how would the thermal properties be influenced if one considered spherical (1a), cylindrical (1b), and ellipsoidal (1c) potentials instead? Despite being an intriguing question, it is challenging to perform such an analysis by analytical means. Nevertheless, this analysis will be performed numerically in an upcoming work.

VII. CONCLUSION AND FUTURE PERSPECTIVES

We examined the behavior of the thermodynamic functions for different geometries, i.e., spherical, cylindrical, and ellipsoidal ones; we primarily used the canonical ensemble for spinless particles. Moreover, *noninteracting* gases were also taken into account for the same geometries with the usage of the grand canonical ensemble description. A study of how geometry affected the system of spinless particles, fermions and bosons was provided as well. We also note that our results could possibly be applied to the *Bose-Einstein condensate* and to the *helium dimer*.

Furthermore, for the bosonic sector, independently of the geometry, the entropy and internal energy turned out to be greater than for the fermionic case; a standard ordering of the sizes of the computed quantities repeatedly occurred for both systems: *Ellipsoid* > *Cylinder* > *Sphere*.

Finally, we constructed a model to provide a description of *interacting* quantum gases; it was implemented for a cubical box. Such an interaction sector turned out to be more prominent since the results were derived analytically. More so, it was possible to estimate the Fermi energy for the cubical box and see how the interaction played the role of modifying it. We also shown how to build an approximated interaction term in order to estimate such energy. Nevertheless, even for the simplest case, we could not obtain analytical results. This aspect clearly demonstrated how intricate were the calculations when we took the interaction into account. Furthermore, another remarkable feature worth exploring, would

be the thermodynamic aspects of anisotropic systems [78].

Acknowledgments

The authors would like to thank João Milton, Andrey Chaves, Diego Rabelo, Ewer-ton Wagner and Paulo Porfírio for the fruitful suggestions during the preparation of this manuscript. More so, we are also indebted to Albert Petrov, Izeldin Ahmed, Marco Schreck, Subir Ghosh, anonymous referee, and the editor for the corrections and recommendations given to this work. Particularly, A. A. Araújo Filho acknowledges the Facultad de Física - Universitat de València and Gonzalo J. Olmo for the kind hospitality when part of this work was made. Moreover, this work was partially supported by Conselho Nacional de Desenvolvimento Científico e Tecnológico (CNPq) - 142412/2018-0, Coordenação de Aperfeiçoamento de Pessoal de Nível Superior (CAPES) - Finance Code 001, and CAPES-PRINT (PRINT - PROGRAMA INSTITUCIONAL DE INTERNACIONALIZAÇÃO) - 88887.508184/2020-00.

-
- [1] D. R. Gaskell and D. E. Laughlin, *Introduction to the Thermodynamics of Materials*. CRC press, 2017.
 - [2] R. DeHoff, *Thermodynamics in materials science*. CRC Press, 2006.
 - [3] B. Mühlischlegel, D. Scalapino, and R. Denton, “Thermodynamic properties of small superconducting particles,” *Physical Review B*, vol. 6, no. 5, p. 1767, 1972.
 - [4] J. W. Tester, M. Modell, *et al.*, *Thermodynamics and its Applications*. Prentice Hall PTR, 1997.
 - [5] C. Lee, W. Yang, and R. G. Parr, “Development of the colle-salvetti correlation-energy formula into a functional of the electron density,” *Physical Review B*, vol. 37, no. 2, p. 785, 1988.
 - [6] A. A. Araújo-Filho, F. L. Silva, A. Righi, M. B. da Silva, B. P. Silva, E. W. S. Caetano, and V. N. Freire, “Structural, electronic and optical properties of monoclinic $\text{Na}_2\text{Ti}_3\text{O}_7$ from density functional theory calculations: A comparison with xrd and optical absorption measurements,” *Journal of Solid State Chemistry*, vol. 250, pp. 68–74, 2017.

- [7] M. E. Casida, C. Jamorski, K. C. Casida, and D. R. Salahub, “Molecular excitation energies to high-lying bound states from time-dependent density-functional response theory: Characterization and correction of the time-dependent local density approximation ionization threshold,” *The Journal of Chemical Physics*, vol. 108, no. 11, pp. 4439–4449, 1998.
- [8] M. D. Segall, P. J. D. Lindan, M. J. a. Probert, C. J. Pickard, P. J. Hasnip, S. Clark, and M. Payne, “First-principles simulation: ideas, illustrations and the castep code,” *Journal of Physics: Condensed Matter*, vol. 14, no. 11, p. 2717, 2002.
- [9] D. C. Langreth and M. J. Mehl, “Beyond the local-density approximation in calculations of ground-state electronic properties,” *Physical Review B*, vol. 28, no. 4, p. 1809, 1983.
- [10] F. L. R. Silva, A. A. A. Filho, M. B. da Silva, K. Balzuweit, J.-L. Bantignies, E. W. S. Caetano, R. L. Moreira, V. N. Freire, and A. Righi, “Polarized raman, ftir, and dft study of na₂ti₃o₇ microcrystals,” *Journal of Raman Spectroscopy*, vol. 49, no. 3, pp. 538–548, 2018.
- [11] A. Imanian and M. Modarres, “Thermodynamics as a fundamental science of reliability,” *Proceedings of the Institution of Mechanical Engineers, Part O: Journal of Risk and Reliability*, vol. 230, no. 6, pp. 598–608, 2016.
- [12] F. Reif, *Fundamentals of statistical and thermal physics*. Waveland Press, 2009.
- [13] A. A. Balandin, “Thermal properties of graphene and nanostructured carbon materials,” *Nature Materials*, vol. 10, no. 8, pp. 569–581, 2011.
- [14] A. Bejan, *Advanced engineering thermodynamics*. John Wiley & Sons, 2016.
- [15] H. Potempa and L. Schweitzer, “Dependence of critical level statistics on the sample shape,” *Journal of Physics: Condensed Matter*, vol. 10, no. 25, p. L431, 1998.
- [16] W.-S. Dai and M. Xie, “Quantum statistics of ideal gases in confined space,” *Physics Letters A*, vol. 311, no. 4-5, pp. 340–346, 2003.
- [17] W.-S. Dai and M. Xie, “Geometry effects in confined space,” *Physical Review E*, vol. 70, no. 1, p. 016103, 2004.
- [18] L. Angelani, L. Casetti, M. Pettini, G. Ruocco, and F. Zamponi, “Topology and phase transitions: From an exactly solvable model to a relation between topology and thermodynamics,” *Physical Review E*, vol. 71, no. 3, p. 036152, 2005.
- [19] D. Braun, G. Montambaux, and M. Pascaud, “Boundary conditions at the mobility edge,” *Physical Review Letters*, vol. 81, no. 5, p. 1062, 1998.
- [20] V. E. Kravtsov and V. I. Yudson, “Topological spectral correlations in 2d disordered systems,”

- Physical Review Letters*, vol. 82, no. 1, p. 157, 1999.
- [21] R. R. Oliveira, A. A. Araújo Filho, F. C. Lima, R. V. Maluf, and C. A. Almeida, “Thermodynamic properties of an aharonov-bohm quantum ring,” *The European Physical Journal Plus*, vol. 134, no. 10, p. 495, 2019.
- [22] R. R. S. Oliveira, A. A. Araújo Filho, R. V. Maluf, and C. A. S. Almeida, “The relativistic aharonov–bohm–coulomb system with position-dependent mass,” *Journal of Physics A: Mathematical and Theoretical*, vol. 53, no. 4, p. 045304, 2020.
- [23] R. K. Pathria, *Statistical mechanics*, vol. 45. Pergamon, 1972.
- [24] L. D. Landau and E. M. Lifshitz, *Statistical Physics: Volume 5*, vol. 5. Elsevier, 2013.
- [25] N. Zettili, “Quantum mechanics: concepts and applications,” 2003.
- [26] H. Weyl, *Gesammelte Abhandlungen: Band 1 bis 4*, vol. 4. Springer-Verlag, 1968.
- [27] D. J. Griffiths and D. F. Schroeter, *Introduction to quantum mechanics*. Cambridge University Press, 2018.
- [28] T. Kereselidze, T. Tchelidze, T. Nadareishvili, and R. Y. Kezerashvili, “Energy spectra of a particle confined in a finite ellipsoidal shaped potential well,” *Physica E: Low-dimensional Systems and Nanostructures*, vol. 81, pp. 196–204, 2016.
- [29] P. A. M. Dirac, *Lectures on quantum mechanics*, vol. 2. Courier Corporation, 2001.
- [30] G. E. Andrews, R. Askey, and R. Roy, *Special functions*, vol. 71. Cambridge university press, 1999.
- [31] R. A. Silverman *et al.*, *Special functions and their applications*. Courier Corporation, 1972.
- [32] W. W. Bell, *Special functions for scientists and engineers*. Courier Corporation, 2004.
- [33] H. Krivine, “Finite size effects on the momentum distribution of non-interacting fermions,” *Nuclear Physics A*, vol. 457, no. 1, pp. 125–145, 1986.
- [34] A. Chaves and D. Neilson, “Two-dimensional semiconductors host high-temperature exotic state,” 2019.
- [35] L. V. Butov, C. W. Lai, A. L. Ivanov, A. C. Gossard, and D. S. Chemla, “Towards bose–einstein condensation of excitons in potential traps,” *Nature*, vol. 417, no. 6884, pp. 47–52, 2002.
- [36] Z. Wang, D. A. Rhodes, K. Watanabe, T. Taniguchi, J. C. Hone, J. Shan, and K. F. Mak, “Evidence of high-temperature exciton condensation in two-dimensional atomic double layers,” *Nature*, vol. 574, no. 7776, pp. 76–80, 2019.

- [37] G. W. Burg, N. Prasad, K. Kim, T. Taniguchi, K. Watanabe, A. H. MacDonald, L. F. Register, and E. Tutuc, “Strongly enhanced tunneling at total charge neutrality in double-bilayer graphene-wse 2 heterostructures,” *Physical Review Letters*, vol. 120, no. 17, p. 177702, 2018.
- [38] S. Chen and P. Tartaglia, “Light scattering from n non-interacting particles,” *Optics Communications*, vol. 6, no. 2, pp. 119–124, 1972.
- [39] V. Degtyarev, S. Khazanova, and N. Demarina, “Features of electron gas in inas nanowires imposed by interplay between nanowire geometry, doping and surface states,” *Scientific Reports*, vol. 7, no. 1, pp. 1–9, 2017.
- [40] L. Bürgi, N. Knorr, H. Brune, M. A. Schneider, and K. Kern, “Two-dimensional electron gas at noble-metal surfaces,” *Applied Physics A*, vol. 75, no. 1, pp. 141–145, 2002.
- [41] H. Lee, N. Campbell, J. Lee, T. Asel, T. Paudel, H. Zhou, J. Lee, B. Noesges, J. Seo, B. Park, *et al.*, “Direct observation of a two-dimensional hole gas at oxide interfaces,” *Nature materials*, vol. 17, no. 3, pp. 231–236, 2018.
- [42] R. Weill, A. Bekker, B. Levit, M. Zhurahov, and B. Fischer, “Thermalization of one-dimensional photon gas and thermal lasers in erbium-doped fibers,” *Optics Express*, vol. 25, no. 16, pp. 18963–18973, 2017.
- [43] X. Liu, J. Zhang, Z. Zhang, X. Lin, Y. Yu, X. Xing, Z. Jin, Z. Cheng, and G. Ma, “Thermodynamics of quasi-2d electron gas at bfo/si interface probed with thz time-domain spectroscopy,” *Applied Physics Letters*, vol. 111, no. 15, p. 152906, 2017.
- [44] C.-X. Zhang, S.-G. Peng, and K. Jiang, “High-temperature thermodynamics of spin-polarized fermi gases in two-dimensional harmonic traps,” *Physical Review A*, vol. 98, no. 4, p. 043619, 2018.
- [45] V. V. Romanov, N. T. Bagraev, V. A. Kozhevnikov, and G. K. Sizykh, “2d electron gas density of states at the fermi level in silicon nanosandwich,” in *Journal of Physics: Conference Series*, vol. 1236, p. 012014, IOP Publishing, 2019.
- [46] D. A. Baghdasaryan, D. B. Hayrapetyan, E. M. Kazaryan, and H. A. Sarkisyan, “Thermal and magnetic properties of electron gas in toroidal quantum dot,” *Physica E: Low-Dimensional Systems and Nanostructures*, vol. 101, pp. 1–4, 2018.
- [47] M. Däne and A. Gonis, “On the v-representability problem in density functional theory: application to non-interacting systems,” *Computation*, vol. 4, no. 3, p. 24, 2016.
- [48] S. Jungblut, J.-O. Joswig, and A. Eychmüller, “Diffusion-and reaction-limited cluster aggre-

- gation revisited,” *Physical Chemistry Chemical Physics*, vol. 21, no. 10, pp. 5723–5729, 2019.
- [49] R. Kutner, “Chemical diffusion in the lattice gas of non-interacting particles,” *Physics Letters A*, vol. 81, no. 4, pp. 239–240, 1981.
- [50] M. Ligare, “Classical thermodynamics of particles in harmonic traps,” *American Journal of Physics*, vol. 78, no. 8, pp. 815–819, 2010.
- [51] M. Wilkens and C. Weiss, “Particle number fluctuations in an ideal bose gas,” *Journal of Modern Optics*, vol. 44, no. 10, pp. 1801–1814, 1997.
- [52] H. Pajkowski and R. Pathria, “Criteria for the onset of bose-einstein condensation in ideal systems confined to restricted geometries,” *Journal of Physics A: Mathematical and General*, vol. 10, no. 4, p. 561, 1977.
- [53] S. Kilić, E. Krotscheck, and R. Zillich, “Binding of two helium atoms in confined geometries,” *Journal of Low Temperature Physics*, vol. 116, no. 3-4, pp. 245–260, 1999.
- [54] S. Kilić, E. Krotscheck, and L. Vranješ, “Binding of two helium atoms in confined geometries. ii. dimerization on flat attractive substrates,” *Journal of Low Temperature Physics*, vol. 119, no. 5-6, pp. 715–722, 2000.
- [55] W. M. Gersbacher and F. J. Milford, “The significance of many-body interactions in physical adsorption,” *Journal of Low Temperature Physics*, vol. 9, no. 3-4, pp. 189–201, 1972.
- [56] E. Zaremba and W. Kohn, “Theory of helium adsorption on simple and noble-metal surfaces,” *Physical Review B*, vol. 15, no. 4, p. 1769, 1977.
- [57] M. Bretz and J. G. Dash, “Quasiclassical and quantum degenerate helium monolayers,” *Physical Review Letters*, vol. 26, no. 16, p. 963, 1971.
- [58] M. Bretz and J. G. Dash, “Ordering transitions in helium monolayers,” *Physical Review Letters*, vol. 27, no. 10, p. 647, 1971.
- [59] M. S. Dresselhaus, G. Dresselhaus, P. C. Eklund, and A. M. Rao, “Carbon nanotubes,” in *The physics of fullerene-based and fullerene-related materials*, pp. 331–379, Springer, 2000.
- [60] A. Jorio, G. Dresselhaus, and M. S. Dresselhaus, *Carbon nanotubes: advanced topics in the synthesis, structure, properties and applications*, vol. 111. Springer Science & Business Media, 2007.
- [61] M. Saarela, B. E. Clements, E. Krotscheck, and F. V. Kusmartsev, “Phase transitions in the growth of 4 he films,” *Journal of Low Temperature Physics*, vol. 93, no. 5-6, pp. 971–985, 1993.

- [62] M. Saarela and F. V. Kusmartsev, “Many-body structure of quantum vortices in thin films,” *Physics Letters A*, vol. 202, no. 4, pp. 317–323, 1995.
- [63] R. Humphries, P. James, and G. Luckhurst, “Molecular field treatment of nematic liquid crystals,” *Journal of the Chemical Society, Faraday Transactions 2: Molecular and Chemical Physics*, vol. 68, pp. 1031–1044, 1972.
- [64] M. W. Klein, “Molecular-field theory of a random ising system in the presence of an external magnetic field,” *Physical Review*, vol. 188, no. 2, p. 933, 1969.
- [65] P. J. Wojtowicz and M. Rayl, “Phase transitions of an isotropic ferromagnet in an external magnetic field,” *Physical Review Letters*, vol. 20, no. 26, p. 1489, 1968.
- [66] D. Ter Haar and M. Lines, “A molecular-field theory of anisotropic ferromagnetics,” *Philosophical Transactions of the Royal Society of London. Series A, Mathematical and Physical Sciences*, vol. 254, no. 1046, pp. 521–555, 1962.
- [67] A. A. Araújo-Filho, F. L. Silva, A. Righi, M. B. da Silva, B. P. Silva, E. W. Caetano, and V. N. Freire, “Structural, electronic and optical properties of monoclinic $\text{Na}_2\text{Ti}_3\text{O}_7$ from density functional theory calculations: A comparison with xrd and optical absorption measurements,” *Journal of Solid State Chemistry*, vol. 250, pp. 68–74, 2017.
- [68] F. L. R. e. Silva, A. A. A. Filho, M. B. da Silva, K. Balzuweit, J.-L. Bantignies, E. W. S. Caetano, R. L. Moreira, V. N. Freire, and A. Righi, “Polarized raman, ftir, and dft study of $\text{Na}_2\text{Ti}_3\text{O}_7$ microcrystals,” *Journal of Raman Spectroscopy*, vol. 49, no. 3, pp. 538–548, 2018.
- [69] A. A. Araújo Filho and A. Y. Petrov, “Higher-derivative lorentz-breaking dispersion relations: a thermal description,” *The European Physical Journal C*, vol. 81, no. 9, pp. 1–16, 2021.
- [70] A. A. Araújo Filho and J. Reis, “Thermal aspects of interacting quantum gases in lorentz-violating scenarios,” *The European Physical Journal Plus*, vol. 136, no. 3, pp. 1–30, 2021.
- [71] A. A. Araújo Filho, “Lorentz-violating scenarios in a thermal reservoir,” *The European Physical Journal Plus*, vol. 136, no. 4, pp. 1–14, 2021.
- [72] A. A. Araújo Filho and R. Maluf, “Thermodynamic properties in higher-derivative electrodynamics,” *Brazilian Journal of Physics*, pp. 1–11, 2021.
- [73] A. A. Araújo Filho and A. Y. Petrov, “Bouncing universe in a heat bath,” *International Journal of Modern Physics A*, vol. 36, no. 34n35, p. 2150242, 2021.
- [74] A. A. Araújo Filho, “Thermodynamics of massless particles in curved spacetime,” *arXiv preprint arXiv:2201.00066*, 2021.

- [75] A. A. Araújo Filho, “Particles in loop quantum gravity formalism: a thermodynamical description,” *arXiv preprint arXiv:2202.13907*, 2022.
- [76] R. Oliveira and A. A. Araújo Filho, “Thermodynamic properties of neutral dirac particles in the presence of an electromagnetic field,” *The European Physical Journal Plus*, vol. 135, no. 1, p. 99, 2020.
- [77] A. A. Araújo Filho, J. A. A. S. Reis, and S. Ghosh, “Fermions on a torus knot,” *arXiv preprint arXiv:2108.07336*, 2021.
- [78] D. Colladay and V. A. Kostelecký, “Lorentz-violating extension of the standard model,” *Physical Review D*, vol. 58, no. 11, p. 116002, 1998.